Journal of the European Ceramic Society 19 (1999) 1895–1901

PII: S0955-2219(98)000268-4
0955-2219/99/$ - see front matter

Ultrasonic Measurement of Young's Modulus MgO/C Refractories at High Temperature

H. Baudson,[a] F. Debucquoy,[a] M. Huger,[a] C. Gault[a]* and M. Rigaud[b]

[a]ENSCI, 47 av. Albert Thomas, 87065 Limoges, France
[b]CIREP, 8475 rue Christophe Colomb, H2M 2N9, Montréal, Québec, Canada

(Received 7 June 1998; accepted 25 October 1998)

Abstract

The paper deals with the elastic behavior of MgO/C refractories used in BOF at temperatures up to 1400°C in air or inert atmosphere. Measurements have been made by the way of a high temperature ultrasonic technique. Heating-cooling cycles and long time aging in the range 700–1400°C show strong variations of Young's modulus which have been interpreted with the aid of XRD analysis, SEM observations and EDS analysis. Carbon oxidation and sintering of MgO particles are found to be responsible of the major parts of the measured evolutions. © *1999 Elsevier Science Limited. All rights reserved*

Keywords: refractories, MgO, carbon, Young's modulus, microstructure: final.

1 Introduction

MgO/C refractories bricks are widely used in steelmaking industry as basic oxygen furnace (BOF) linings because of their good resistance both to slag corrosion and to thermal stresses.[1] But the efficiency of these refractories is highly dependent on the conservation in service (i.e. at $T \geq 1600°C$) of the carbon phases.[2] At $T > 1400°C$, oxido-reduction mechanisms between carbon and magnesia are responsible of the formation of a dense MgO zone at the surface of the bricks.[3] This is fundamental because it inhibits the carbon consumption in service at high temperature and increases the protection against slag penetration. Unfortunately decarbonization at rather low temperatures (above 600°C) in presence of oxygen can occur, which consequence is an evolution of the composition and of the microstructure of the material during heating the lining up to the temperature of service:

- the consumption of carbon from the surface towards the core of the material involves a time-dependent carbon concentration gradient trough the thickness of the bricks;
- this is accompanied by an increase of porosity, in particular at the surface of the bricks.

Therefore the prediction of life times of the bricks in service, which is generally based on numerical calculations of stress fields in the linings, previously needs the knowledge of these evolutions (mechanisms and kinetics) in order to determine their impact on the thermomechanical parameters which are used for modelling.

Most of microstructural evolutions (densification, phase changes, crystallization, etc.) and of damage (microcracking) occuring in materials involve variations of the effective Young's modulus E. Consequently, ultrasonic measurements of E at high temperature can be used to monitor such evolutions in numerous ceramics.[4] This paper deals with results obtained in MgO–C refractories in the range 20–1400°C in air or argon at atmospheric pressure, using an ultrasonic technique adapted to the case of highly heterogeneous materials. An attempt is made to understand the structural changes responsible of Young's modulus variations, by correlations with results of thermogravimetric analysis (TGA), thermal expansion measurements, characterizations by XRD and EDS analyses, and SEM observations.

*To whom correspondence should be addressed.

2 Experimental Details

2.1 Material

MgO/C bricks were prepared by NARCO* by mixing sea water magnesia particles (96·5% MgO, 2·2% CaO, 0·31% SiO_2, 0·2% Fe_2O_3, 0·15% $A1_2O_3$, 0·01% B_2O_3) and natural graphite flakes (94% C, 5% ash with SiO_2 and Al_2O_3 as main impurities, 1% volatiles) into a liquid phenolic resin acting as a binder, followed by uniaxial pressing. Parallelepipedic samples ($10\times15\times100\,mm^3$) for ultrasonic experimentation were cut from the bricks in the as-pressed state using a diamond saw.

Figure 1 shows a picture obtained by SEM observations of a sample cross section. EDS analysis was used to identify the elements and revealed a highly heterogeneous texture with a wide distribution of MgO particles: fine MgO particles (inferior to 5 μm) are packed between large particles (more than 500 μm for the largest ones), surrounded by a mixture of graphite platelets and resin.

Before measurements, the samples were carbonized for 5 h at 1000°C in a CO atmosphere in order to pyrolyse the resin.[5] The resulting material (taken as the starting state for experimentation) is a composite of MgO particles embeded in carbon (graphite platelets and secondary pyrolytic carbon) and a significant amount of porosity (about 13%). Additionally, cracks and secondary phase coming from impurities have been observed in pyrocarbon (Fig. 2). Table 1 gives the main characteristics of the material in the as-pressed state and in the carbonized state.

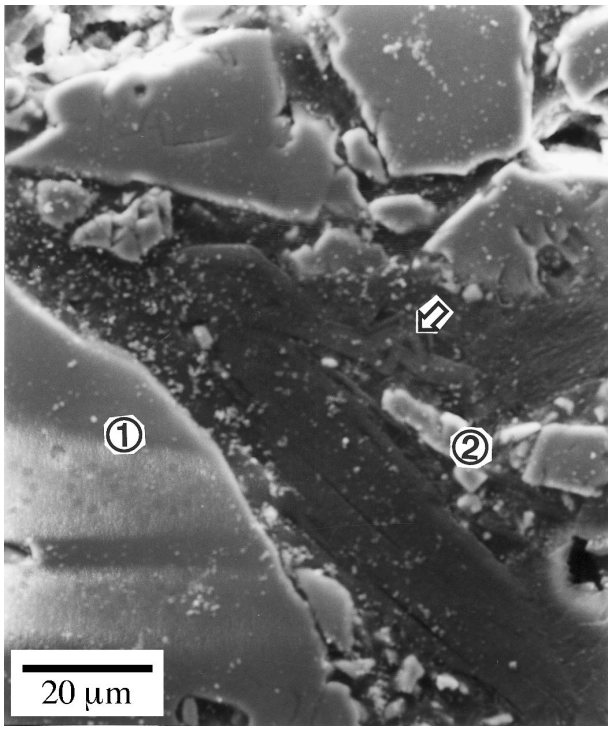

Fig. 1. SEM picture of a polished cross section of as-pressed MgO/C: ① large MgO particles; ② small MgO particles; graphite platelets (arrow) embedded in phenolic resin.

*NARCO: North American Refractories Co, Cleveland, OH. 44115, USA.

2.2 Technique used for high temperature ultrasonic measurements

Ultrasonic measurements of Young's modulus at high temperature have been performed using a pulse-echo method in a 'long bar mode'. The principle of such measurements has been reported elsewhere.[4] The frequency and the geometry of the ultrasonic line have been adapted to take into account the particular texture of refractories with large grains (up to 5 mm) and high porosity (up to 20%), which involves very low elastic properties and high ultrasonic attenuation. Figure 3 schematically shows the device with the associated echo pattern.

Wideband pulses of ultrasonic compressional waves, with a 30 kHz central frequency, are generated by a magnetostrictive tranducer and propagate through the rectangular sample via two waveguides. All parts of the ultrasonic line are attached together by a refractory cement. For propagation in long bar mode, the wavelength must be larger than the cross dimensions of the propagation medium. The diameter of the alumina waveguide is

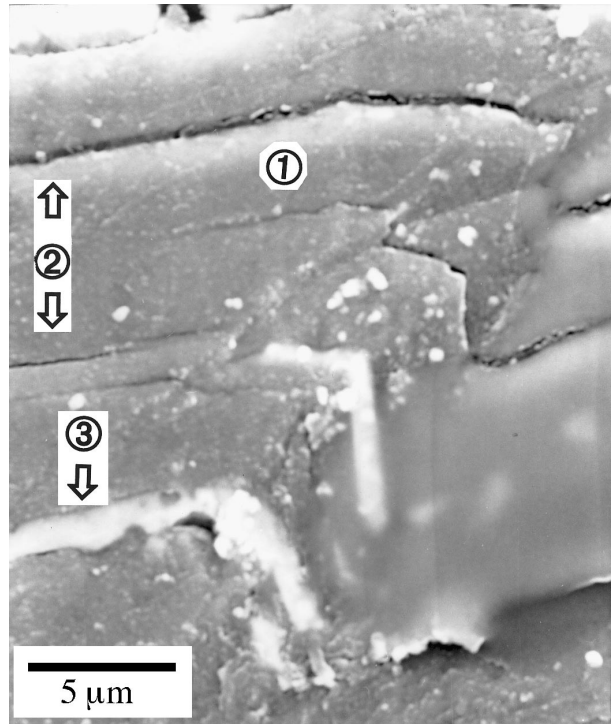

Fig. 2. SEM picture of a polished cross section of MgO/C after carbonization: details of graphite flake ①, bent, partially exfoliated (cracks ②) with secondary phases ③ related to the minerals attached to or associated with the flake.

Table 1. Composition and characteristics at 20°C of the studied MgOC refractory

Material state	*MgO (wt%)*	*Carbon (wt%)*	*Density (kg m^{-3})*	*Apparent porosity (%)*	*Young's modulus (GPa)*
As-pressed	89.8[(N)]	8.0[(N)]	3000[(N)]	6.7[(N)]	—
Carbonized	89.8[(N)]	6.5[(N)]	2880[(P)]	13.1[(N)]	5–7[(P)]

[(N)] given by NARCO.
[(P)] determined in the present work.

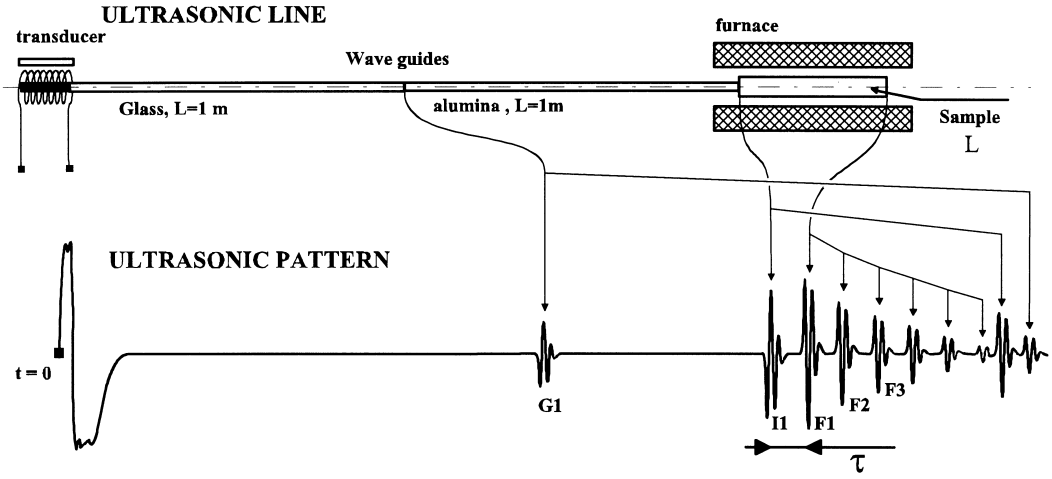

Fig. 3. Principle of ultrasonic Young's modulus measurement at high temperature.

10 mm and samples have a rectangular section of $10\times15\,mm^2$. The ultrasonic line is vertically fitted in a gas tight alumina tube into a 1700°C furnace for high temperature measurements in controlled atmosphere (air or inert gas). An electronic device, described elsewhere,[6] automatically measures and records the time t between two successive echoes in the sample. The longitudinal ultrasonic velocity V in the long bar mode, is then given by:

$$V = 2L/t \tag{1}$$

and Young's modulus E by:

$$E = \rho V^2 \tag{2}$$

where L and ρ are sample length and density, respectively.

Length variations caused by thermal expansion or mass variations induced by chemical reactions during heating have to be taken into account for accurate measurements. Corrections can be made from TGA and dilatometric experiences performed in similar conditions.[6]

3 Results and Discussion

3.1 Young's modulus variations during monotonic temperature cycles

Figure 4 shows the relative variations of Young's modulus $(E-E_0)/E_0$ (E_0 being the value measured at 20°C in the carbonized state) observed in two samples of the same MgO/C refractory, during temperature cycles between 20 and 1400°C with heating/cooling rates of 5°C min^{-1}. One sample was heated twice in air: first cycle (curve 'Air1') with a 30 min dwell at 1400°C, and second cycle (curve 'Air2') with a 1 h dwell at 1400°C. Another sample was heated in argon (curve 'Ar') with a 1 h dwell at 1400°C. No corrections versus thermal expansion or mass variations were made because they were found to be inferior to 5% in the whole temperature range which is negligible compared with the observed variations. When cooling, the cement between the waveguide and the sample generally broke because of differential thermal contraction. Then a new cementation was necessary to determine the final value at room temperature after each cycle.

Whatever the atmosphere, the $(E-E_0)/E_0 = f(T)$ curves are not linear as they usually are for stable ceramics and roughly exhibit the same aspect with an unreversible increase above 850°C and during the temperature dwells at 1400°C. After cooling, a permanent Young's modulus augmentation of more than 50% compared with E_0 is observed in all cases.

Young's modulus of graphite is known to have a non linear behaviour versus temperature with an increase up to 1000°C after a minimum at 200–400°C,[7] though MgO exhibits a regular decrease.[8] A simple calculation with a mixture law shows that, because of the low carbon fractional volume

(~9%), the intrinsic effect of the variation of Young's modulus of C versus temperature is negligible (~6%) compared with the effect of the variation of Young's modulus of MgO (~94%). Then it cannot explain the non-linearity of the $(E - E_0)/E_0 = f(T)$ curves with increasing temperature.

Therefore other mechanisms, depending on atmosphere and temperature, were considered to interprets the curves of Fig. 4. They have been identified by correlation with results of SEM observations, EDS and XRD analysis before and after heat treatments.

1. Thermomechanical effects associated to the differential thermal expansion of the constituents, in particular between carbon strates (graphite and pyrocarbon) with a strongly anisotropic thermal expansion behavior and large magnesia particles with a high thermal expansion. This effect results in cracks and decohesions which are observed in the starting carbonized state (Fig. 2) and can lead to hysteretic effects on $E=f(T)$ curves as it is classical in large grained ceramics.[9] Crack closure occurs on heating, leading to an increase of E (above 800°C for curves 'Air 1' and 'Ar') and crack opening can involve a decrease when cooling (for example below 700°C for curve 'Ar'). These mechanisms can be modified by others, namely oxidation of carbon phases and/or sintering, which can be responsible of porosity variations, grain growth and crack healing at high temperature.
2. Oxidation of carbon phases occurs in air above 600°C as it has been found by TGA experiments performed in conditions similar to ultrasonic measurements: a mass loss was observed above 600°C and a decrease of the carbon peak was found by XRD performed after TGA experiments. Then, the drop observed between 600°C and 850°C on curve 'Air1' in Fig. 4, which is not present in argon, can be attributed to the porosity created by carbon burnout.
3. An increase of Young's modulus was observed during the dwells at 1400°C in both air and Ar. Furthermore, when cooling after the first run in air, E regularly increases and closely follows the same $E=f(T)$ curve as for a dense sintered magnesia.[8] This suggests a densification mechanism which could result of MgO–C interaction in oxygen at high temperature leading to the formation of a dense MgO zone at the surface.[2] The plot in Fig. 5 of the variations of E versus the cumulated time during the dwells at 1400°C, is consistent with the hypothesis of a densification process: the variation of E during the second run follows the same law than the variation during the first run. But the measured variations being more important in Ar than in air and 1400°C being rather low for the decomposition of MgO, the asumption of MgO–C interaction is not valuable. Therefore densification should be attributed to sintering of particles in MgO agglomerates, maybe favoured by intergranular phases formed by impurities.

When cooling after the second run in air (Air2) and after the run in argon (Ar), the curves follow, in a first time, the same $E=f(T)$ variations as for a dense sintered magnesia (like for curve Airl), but drop below 800°C. This effect is more significant for the treatment under Ar which leads to the highest value of E after the dwell at 1400°C (more than 100% of increase), denoting achievement of a high densified state with large sintered MgO agglomerates, which is favorable for cracking when cooling.

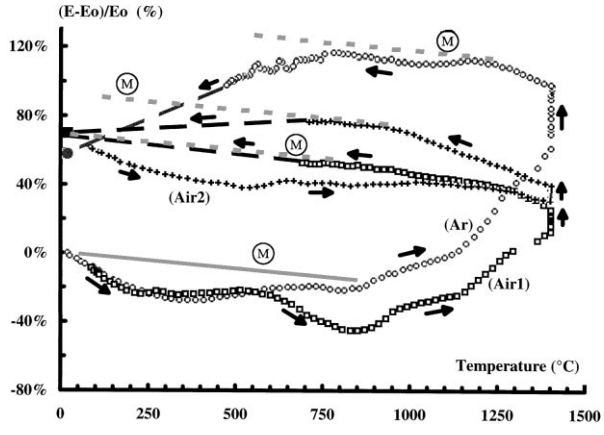

Fig. 4. Young's modulus variations versus temperature normalized to room temperature value E_0. (Temperature variation rate: 5°C min^{-1}). (Air 1): 1st cycle in air; (Air2): 2nd cycle in air; (Ar): cycle in argon; (M): variations for dense MgO, after Ref. 8.

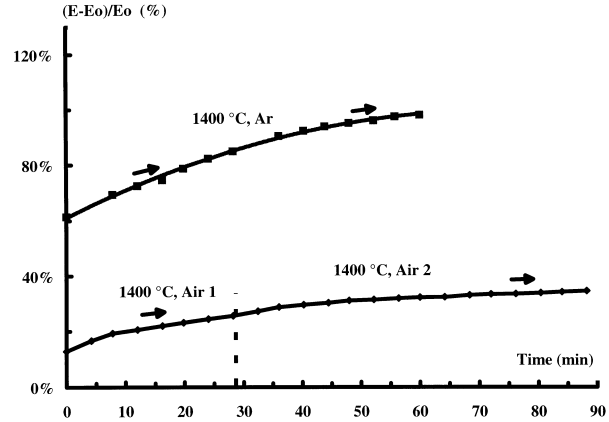

Fig. 5. Variations of Young's modulus versus time during the isothermal agings of Fig. 4 at 1400°C in air and in Ar. E_0 is the initial value of E at 20°C. Time t=0 for the 2nd dwell in air corresponds to the end of the 1st dwell in air (~30 min).

In order to confirm these interpretations—oxydation of carbon at low temperature and sintering of magnesia at high temperature—isothermal treatments have been performed under various atmosphere conditions.

3.2 Aging at intermediate temperature: carbon oxidation

Variations of Young's modulus have been measured during isothermal aging at 700°C, first in nitrogen (after heating under nitrogen) for 2 h, and then in air. The curve of Fig. 6 shows a drop when air is introduced. After 2 h in air at 700°C, E remains constant which denotes the stability of the material. As it was mentionned above, mass losses are observed at this temperature, which suggests that carbon burnout occurs and may be the cause of Young's modulus decrease because of an augmentation of porosity. As oxydation of graphite is rather low at 700°C in air, this effect should be attributed to the oxydation of pyrocarbon formed by pyrolysis of the resin during carbonization. This is confirmed by SEM observations, EDS and XRD analyses of a cross section of the sample after aging at 700°C which confirm that graphite platelets are still present in the material.

3.3 Aging at 1200°C: sintering of MgO particles

The two curves 'Air 1' and 'Ar' in Fig. 4 exhibit an increase of their slope between 1100°C and 1300°C. A thermal expansion experiment performed in air shows that a shrinkage of about 0.4% occurs above 1150°C (Fig. 7). Therefore, isothermal agings at 1200°C have been performed in argon in order to study whether a sintering mechanism could be observed in this temperature range; the results are given in Fig. 8. As at 1400°C, two temperature runs have been made, with a first dwell of 5 h at 1200°C, then cooling down to 20°C and, after a new cementation of the sample to the waveguide, a second heating up to 1200°C. In both cases, Young's modulus increases versus time. The relative variations $(E - E_i)/E_i$ (E_i being the value at the beginning of the dwell) are similar for the two agings up to 5 h. Then a continuous increase of E is observed during the second aging up to 90 h without achievement of any steady state. After this heat treatment, the material exhibits at room temperature a Young's modulus of about 17 GPa which is approximately 3 times the value of E_0 in the carbonized state (cf. Table 1).

As it was expected in a non oxidizing atmosphere, XRD analysis of the aged material gives the same MgO and C peaks as in the carbonized state. But SEM pictures of a polished cross section clearly showed large dense MgO domains formed of sintered grains (Fig. 9), which were never observed in the starting material. Then, though the temperature range is much lower than the usual one for MgO densification, a sintering mechanism seems to occur in MgO aggregates, probably favoured by a significant amount of intergranular phases containing Al_2O_3, SiO_2, CaO impurities which were detected by EDS analysis.

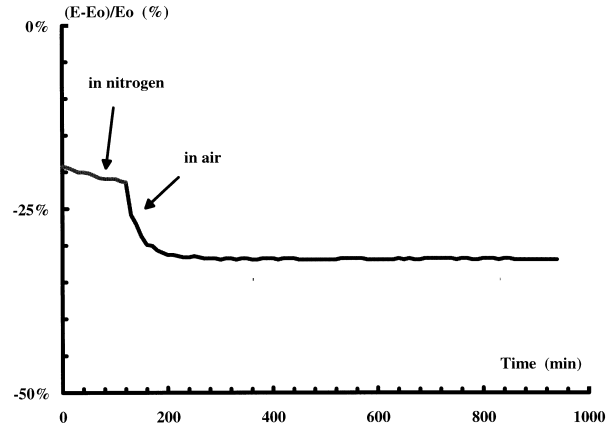

Fig. 6. Young's modulus variations, normalized to the initial value E_0 at 20°C, during aging at 700°C, first in N_2, then in

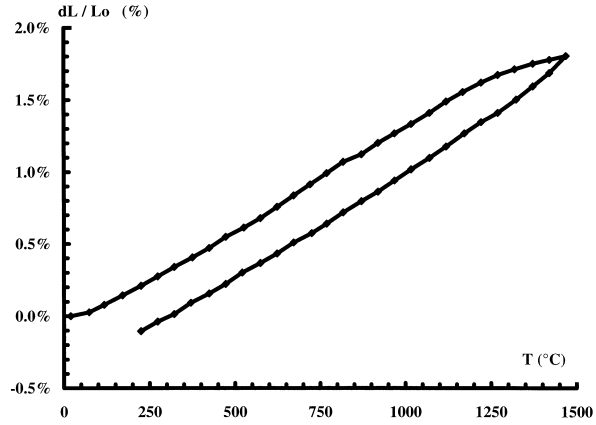

Fig. 7. Thermal expansion measurement between 20 and 1450°C in air at 300°C h^{-1}.

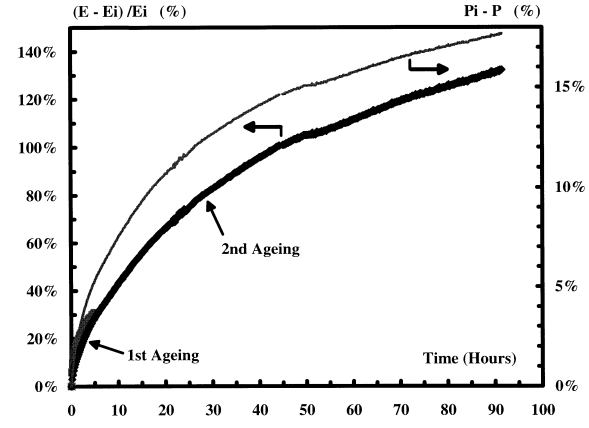

Fig. 8. Relative variations of Young's modulus versus time during two isothermal agings at 1200°C in argon. E_i is the value of E at the beginning of each dwell (t=0). Corresponding porosity decrease into magnesia aggregates calculated from eqn (7).

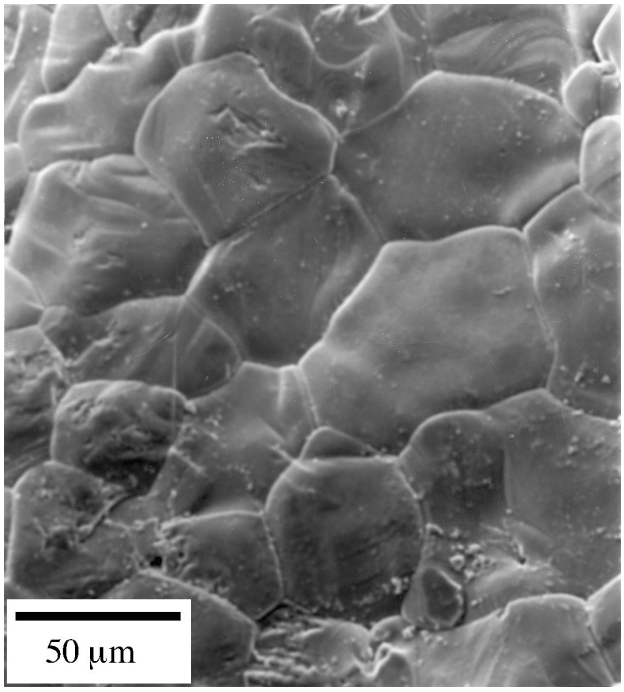

Fig. 9. SEM picture of a large domain of MgO sintered particles in a polished cross section of the sample aged 100 h at 1200°C in Ar.

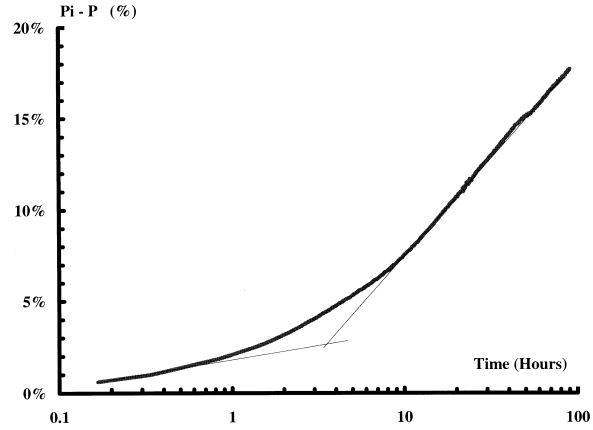

Fig. 10. Plot of the decrease of porosity $P_i - P(t)$ versus Log t into magnesia aggregates.

The increase of Young's modulus can be related to the decrease of porosity into MgO aggregates. The very low value of E in the carbonized state is explained by the weak bonding of the stiff particles (MgO and graphite) by pyrocarbon and secondary phases, with cracks and pores. The fractionnal volumes of carbon and of magnesia in the starting material are approximately 9 and 72% respectively. Then, the major contribution to the stiffness of the material comes from magnesia which additionally has the higher Young's modulus (~300 GPa/~180 GPa for graphite). Therefore, Young's modulus E of the refractory can be written as:

$$E = \delta E_M \tag{3}$$

where E_M is Young's modulus of the magnesia aggregates with porosity P, and $\delta << 1$ is a coefficient depending on the individual elastic properties and on the geometrical arrangement of the constituents arround the magnesia aggregates.

The dependence of Young's modulus on porosity in ceramics has been extensively investigated both by experimental and theoretical approaches. In the case of MgO, Spriggs *et al.*[10] have compiled a lot of experimental data from different authors and they found that the variation of E_M versus porosity could be expressed by an empirical law:

$$E_M = E_{M0} \exp(-bP) \tag{4}$$

with E_{MO} Young's modulus of a fully dense MgO polycrystal and b an empirical constant equal to 4.74 for MgO.

More recent works[11] have derived this exponential relationship using a model of ellipsoidal pores characterized by a shape ratio $k = c/a$ (c and a being the two main axes of the ellipsoid), with random or prefered orientation. For random orientation it has been demonstrated that b is a function of Poisson's ratio v and of k. For $v = 0{\cdot}25$ it gives $b = 2{\cdot}3$ for $k = 1$ (spherical pores) and $b > 2{\cdot}3$ when $0 < k < 1$. Then the value of b determined for MgO from experimental results is consistent with this analysis and have been taken for our discussion.

Using eqns (3) and (4), Young's modulus of the refractory, E_i, at the beginning of isothermal aging at 1200°C can be written:

$$E_i = \delta E_{MO} \exp(-bP_i) \tag{5}$$

where P_i is the average porosity in the magnesia aggregates at the beginning of aging.

Assuming that during the isothermal heat treatment in non oxidizing atmosphere, the only microstructural change is densification by bridging of MgO grains in magnesia aggregates, δ can be assumed to be constant with time. Then at time t:

$$E(t) = \delta E_{MO} \exp[-bP(t)] \tag{6}$$

The decrease of porosity versus time in magnesia aggregates involved by sintering at 1200°C can be derived from the experimental result $(E - E_i)/E_i = f(t)$ of Fig. 8 from eqns (5) and (6) (with $b = 4.74$):

$$\Delta P(t) = P_i - P(t) = 0{\cdot}21 \times \mathrm{Log}\left[\frac{E(t) - E_i}{E_i} + 1\right] \tag{7}$$

The decrease of porosity calculated with eqn (7) during the second aging at 1200°C in Ar up to 90 h is plotted on the same Fig. 8. It must be noted that the signification of this curve is only qualitative: it shows that, about 17% of densification into the magnesia aggregates could explain the increase of 130% in Young's modulus after aging 90 h at 1200°C. A more rigourous evaluation would require the knowledge of the pore distribution and shape in the aggregates for the determination of b.

Moreover, as it was mentionned above, the distribution size of MgO particles is very wide and different pore-size sintering regimes are expected, as it was demonstrated by Sacks *et al.* in mullite.[12] These authors have shown that for a simple cubic packing arrangements of particles of different sizes, different densification regimes can be observed corresponding to successive straight lines with different slopes on a plot $\%\rho_{th}$ versus Log t: the first regime with the lowest slope corresponds to sintering of the smallest particles, the highest slope corresponds to sintering of the largest particles in the distribution. The plot of $\Delta P(t) = f(\mathrm{Log}t)$ in Fig. 10 is clearly characteristic of a densification mechanim of an heterogeneous medium.

4 Conclusion

Ultrasonic measurement at high temperature of Young's modulus of MgO/C refractories allowed two important conclusions:

- pyrocarbon burn-out occurs when heating in air, in particular in the 600–800°C range where a decrease of the average Young's modulus of approximately 10% is observed;
- above 1100°C, a densification by bridging of MgO grains into the magnesia aggregates can involve very important increases of Young's modulus (~130% after 90 h at 1200°C in Ar) and probably, contribute to limit the oxygen access towards the core of the material.

Additional investigations are now necessary to understand the mechanism of sintering of MgO in a rather low temperature range (in particular the role of impurities) and to determine whether an equilibrium can be reached for long time at high temperature in air.

References

1. Peretz, I. and Brezny, B., Magnesia-graphite refractories for BOF converters. *Am. Ceram. Soc. Bulletin*, 1992, **71**(9), 1383–1390.
2. Brezny, R. and Semler, C. E., Oxidation and diffusion in selected pitch-bonded magnesia refractories. *J. Am. Ceram. Soc.*, 1984, **67**(7), 480–483.
3. Pickering, G. D. and Bachelor, J. D., Carbon–MgO reactions in BOF refractories. *Am. Ceram. Soc. Bulletin*, 1971, **50**(7), 611–614.
4. Gault, C., Ultrasonic non destructive evaluation of microstructural changes and degradation of ceramics at high temperature. *Am. Mater. Res. Soc. Symp. Proc.*, 1989, **142**, 263–274.
5. Li, X., Rigaud, M. and Palco, S., Oxidation kinetics of graphite phase in magnesia–carbon refractories. *J. Am. Ceram. Soc.*, 1995, **78**(4), 965–971.
6. Lamidieu, P. and Gault, C., Improved ultrasonic measurement of Young's modulus at high temperatures in composite materials. Application to refractory concretes. *Mater. Sci. Eng. Letter*, 1986, **77**, L11–L15.
7. Mason, I. B. and Knibbs, R. H., Variation with temperature of Young's modulus of polycrystalline graphite. *Nature*, 1960, **188**, 33–35.
8. Soga, N. and Anderson, O. L., High-temperature elastic properties of polycrystalline MgO and $A1_2O_3$. *J. Am. Ceram. Soc.*, 1966, **49**(7), 355–359.
9. Case, E. D., Smyth, J. R. and Hunter, O. Jr, Microcracking in large-grain $A1_2O_3$. *Mater. Sci. Eng.*, 1981, **51**, 175–179.
10. Spriggs, R. M., Brissette, L. A. and Vasilos, T., Effect of porosity on elastic and shear moduli of polycrystalline magnesium oxide. *J. Am. Ceram. Soc.—Discussions and Notes*, 1962, **45**(8), 400.
11. Andersson, C. A., Derivation of the exponential relation for the effect of ellipsoidal porosity on elastic modulus. *J. Am. Ceram. Soc.*, 1996, **79**(8), 2181–2184.
12. Sacks, M. D. and Pask, J. A., Sintering of mullite-containing materials: II, effect of agglomeration. *J. Am. Ceram. Soc.*, 1982, **65**(2), 70–77.